International Journal of Marine Engineering Innovation and Research, Vol. 10(2), June. 2025. 574-583
(pISSN: 2541-5972, eISSN: 2548-1479)

The Effect of Manhole Form on Double Bottom Ship Construction

Rudianto[1*], Ede Mehta Wardhana[2] , Jangka Rulianto [3], R Puranggo Ganjar Widityo[4], Ansori[5]
(Received: 11 May 2025 / Revised: 5 June 2025 /Accepted: 23 June 2025 / Available Online: 30 June 2025)

***Abstract*—The ship's hull construction must withstand all loads, be made as light as possible and comply with regulations. The purpose of this study was to determine the maximum strength limit of double bottom ship construction with manhole form variations. Research design for this study; literature studies, field studies, and simulations using ANSYS. The results of the existing double model structure strength values for the maximum stress values in the sagging hogging state are 236.60 MPa and 154.18 MPa. Von Mises stress values are 227.94 MPa and 136.26 MPa. The shear stress values are 131.5 MPa and 77.36 MPa. The maximum deformation is 0.0049 m, and the safety factor is 1.346. The total construction weight is 201.83 metric tons. The best results of the analysis of variation were found in Model B1, which changed the hole ratio from 0.75 to 0.6 and increased the hole dimension by 200 mm. The maximum stress values of Model B1 in the sagging-hogging condition are 186.93 MPa and 141.54 MPa. Von Mises stress values are 238.72 MPa and 184.82 MPa. The shear stress values are 113.37 MPa and 137.42 MPa. The safety factor is 1.337 m, and the maximum deformation is 0.0034 m.**

Keywords— Manhole, double bottom, strenght

I. INTRODUCTION

The ship's hull is composed of a collection of steel plates and profiles that are designed according to the plan so that they are formed into one unified part. The construction complies with regulatory standards if it can withstand all working loads and is planned to be as light as possible without reducing the strength limits set by the classification agency [1]. To reduce the weight of the construction, engineering was carried out in the form of making holes in the double-bottom solid floor plates. The addition of holes in the construction plate will reduce the cross-sectional area of the plate so that the maximum stress on the plate will also be reduced. In contrast to intact structures, stress analysis for hollow types of structures has not been studied extensively [2].

This study aims to determine the results of the analysis of the maximum strength of the ship's double bottom construction due to manhole variations in accordance with the regulations of the Indonesian Classification Bureau, as well as obtain the most efficient value of the strength and weight of the double bottom construction.

Rudianto. Naval Architecture, University of Jember, Jember, 68121, Indonesia. E-mail: rudianto@unej.ac.id
Ede Mehta Wardhana. Marine Engineering, Institut Teknologi Sepuluh Nopember, Surabaya, 60111, Indonesia. Email: ede@ne.its.ac.id
Jangka Rulianto. Ship Manufacture Engineering, Politechnic State Banyuwangi, Banyuwangi, 68461, Indonesia. Email: jangka.rulianto@poliwangi.ac.id
R. Puranggo Ganjar Widityo. Naval Architecture, University of Jember, Jember, 68121, Indonesia. E-mail: ganjarwidi.teknik@unej.ac.id
Ansori. Naval Architecture, University of Jember, Jember, 68121, Indonesia.. E-mail: ansorigl209@gmail.com

II. METHOD

This research is planned to use quantitative methods. The research designs that will be used to compile this research are literature studies, field studies, and simulations using software. Literature studies originate from classification rules, journals, books, and other media. Exploring related literature and identifying problems with the object to be studied constitutes literature study. In addition, literature studies are also focused on understanding research-related material and providing a basis for planning the sequence of research steps. The field study was carried out by observing the shipyard company. Field studies were conducted to obtain the data used in the research. The types of data used in this research are primary data and secondary data. Primary data comes from observations in the company, while secondary data is data from manual calculations that are the result of primary data processing. Primary data includes information on the main dimensions of the ship, midship construction design, and material specifications. Meanwhile, secondary data includes the results of calculations and planning for construction loads, the detailed design of variation forms, and boundary conditions. Primary research data can be seen in Table 1 and Figure 1 below:

From the primary data, we carried out the calculation of the load. The load used is the weight of the construction and the hydrostatic pressure of seawater. The construction weight is obtained by the method of detailing the construction components. Meanwhile, the hydrostatic pressure experienced by an object in the fluid is caused by the gravitational force of the fluid above that point [3]. To apply pressure and with various draft values, the hydrostatic pressure at any point along the ship is calculated using the equation ($P = \rho . g . h$) [4]. Meanwhile, based on BKI Vol. II Section 5 F.1.2 of 2022 concerning loads on the tank structure, it is explained that the amount of pressure due to dynamic

waves is directly proportional to the vertical motion component, where this loading is calculated by the equation:

$$P = \rho \, .g \, . \, h \, . \, aZ \qquad (1)$$

Where aZ is the vertical component of the calculation results.

After obtaining the load value, an analysis of the modification of the manhole model is carried out as the object of research. The basis for planning the variation of the model is BKI Sec. 8 and Sec. 23 regarding manholes [5]. A variable one is made with a scale measuring the number of holes to determine the effect of the number of manholes on the strength of the double bottom construction [6]. The second variable is made with a measurement scale of the ratio of diameter to length or height of the hole to determine the effect of manhole dimensions on the strength of the double bottom construction [7], variable three is made with a scale measuring the effect of the number and ratio of manhole sizes to determine the effect of the dimensions and number of manholes on the strength of the double bottom construction. From this plan, nine variations of the existing model were obtained.

TABLE 1.
PRINCIPAL DIMENSION

Description	Size
Type	*oil tanker*
Length all/LOA (meters)	157
length LBP (meters)	149.5
Breadth/B (meters)	27.7
High/H (meters)	12
Draft/D (meters)	7
Speed/Vs (Knot)	13
Construction system	longitudinal

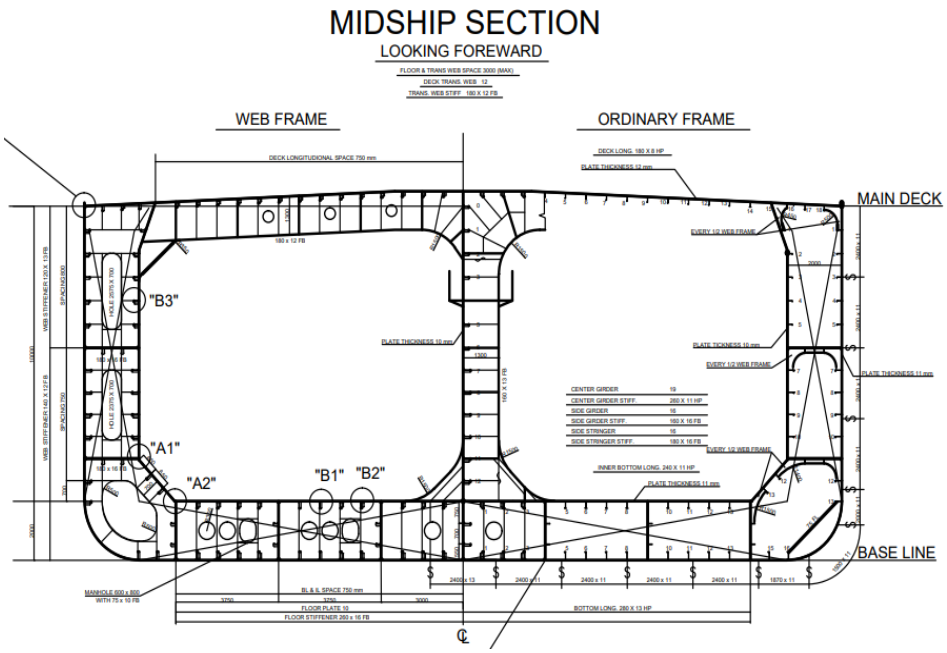

Figure 1. Design construction midship

The simulation is carried out using finite element-based software, and the analysis has the following process sequence:

A. Engineering Data

Process of defining the specifications for input materials. Material specifications are input based on the primary data that has been obtained. Material specifications can be seen in Table 2 below:

TABLE 2.
MATERIALS SPECIFICATION

Description	Size
Ultimate tensile yield (MPa)	307
Ultimate tensile Stress (MPa)	428
Elongation	0.28
Modulus Elastisity (MPa)	2.0×10^5

B. Geometry

Process of inputting the design model into the project schematic or work screen. In this process, validation is also carried out to determine whether the model created is solid so that errors do not occur during the meshing process.

C. Meshing

Stage of converting the discrete geometry model into finite elements and node points to be analyzed [8]. In this process, model convergence is also carried out. The purpose of the convergence model is to measure the accuracy of the software so that the results of the simulations are valid. Convergence is done by comparing the results of the analysis of several element sizes (meshing). Convergence is achieved when the value of the analysis results is stable between the sizes of one element and the sizes of other elements [9].

D. Setup

Boundary conditions are used on structures to provide support or boundary conditions [10]. Assuming boundary conditions in finite element calculations or model analysis must be arranged in such a way that the loading is as similar as possible to real conditions [3]. Boundary conditions are assigned to the independent points at both ends of the model. The independent point is the neutral axis of the model in that area. For nodes around the independent point, a rigid link is defined [10]. Rigid links are picked up on the floor plates at both ends of the model. Meanwhile, load conditions are given to the base plate and inner bottom plate, support plates, girders, bilges, longitudinal members, and brackets. Boundary condition planning can be seen in Table 3 below:

TABLE 3.
BOUNDARY CONDITION

Independent point	*Sagging*			*Hogging*		
	x	y	z	x	y	z
After	-	√	√	-	-	-
Middle	√	√	√	√	√	√
Fore	√	√	√	√	-	-

E. Solution

The desired simulation output setup process.

F. Solve

Active process that displays (reports) simulation results.

After doing the simulation, the next step is validation and analysis of the conclusions. Validation is based on three factors: the safety factor, allowable stress, and validation between simulation results and manual calculation results. The maximum stress is said to be valid if it does not exceed the allowable stress. The safety factor requirement meets the rules if it has a value of more than one [11]. The safety factor value for vertical flexural strength is 1.1 for the sagging condition and 1.2 for the hogging condition [12]. Meanwhile, the validity between engineering mechanics calculations and software analysis should not be more than 0.2 [13]. The allowable stress based on BKI Volume II Section 5 D.1.2 of 2017 is as follows:

$$\sigma_{permit} = 190/k \quad (2)$$

Where k is a material factor (0.77) derived from the BKI Section 2 B.1.4 calculation. After the validation is carried out, the results and conclusions are analyzed.

III. RESULTS AND DISCUSSION

A. Results

The results of the calculation construction load based on the breakdown method are as follows:

Deck construction weight	:	67.912 tons
Side construction weight	:	144.280 tons
Bulkhead construction weight	:	30.260 tons
Bilge construction weight	:	44.928 tons

From the load data above, add the double bottom weight for each model so that the weight data is obtained in Table 4 below:

TABLE 4.
LOAD CONSTRUCTION

Model	m (ton)	g (m/s^2)	W (kN)	A (m^2)	P (Pa)
existing	489.210	9.807	4797.5	476.21	10074
A1	489.148	9.807	4796.9	518.88	9244.7
A2	489.120	9.807	4796.6	518.04	9259.2
A3	488.781	9.807	4793.3	512.40	9354.6
B1	488.912	9.807	4794.6	518.04	9255.3
B2	487.454	9.807	4780.3	517.1	9244.4
B3	487.305	9.807	4778.8	515.92	9262.7
C1	488.856	9.807	4794	516.36	9284.3
C2	486.875	9.807	4774.6	516.8 9	9237.1
C3	486.652	9.807	4772.4	515.47	9258.4

Meanwhile, results calculating seawater hydrostatic pressure based equation 1 are as follows:

P = 1025 kg/m^3 x 9,801 m/s^2 x 2 m x 0,0008
P = 16,09 kN/m^2
P = 1609 Pa

The simulation results for each model of the sagging and hogging conditions can be seen in Tables 5 and 6 below:

TABLE 5.
SIMULATION RESULT SAGGING CONDITION

Model	σ maks (MPa)	σ vm (MPa)	σ shear (MPa)	Deformation (m)	*Safety Factor*
Existing	236.600	227.940	131.500	0.005	1.346
A1	234.050	274.760	157.800	0.013	1.117
A2	189.870	190.720	97.590	0.002	1.600
A3	208.680	272.560	156.420	0.002	1.126
B1	186.930	238.720	137.420	0.003	1.337
B2	157.960	223.880	128.760	0.003	1.116
B3	125.770	248.500	143.120	0.002	1.230
C1	184.120	195.200	112.360	0.002	1.570
C2	159.850	248.480	143.040	0.002	1.235
C3	175.010	236.830	136.440	0.002	1.290

TABLE 6.
SIMULATION RESULTS HOGGING CONDITION

Model	σ maks (MPa)	σ vm (MPa)	σ shear (MPa)	Deformation (m)	*Safety Factor*
Existing	154.180	136.260	77.360	0.001	2.253
A1	256.740	242.180	139.580	0.012	1.260
A2	147.430	159.470	119.080	0.003	1.920
A3	162.620	183.320	105.060	0.002	1.674
B1	141.540	184.820	113.370	0.002	2.119
B2	203.010	252.290	145.180	0.002	1.216
B3	83.600	106.520	61.470	0.002	2.882
C1	177.100	187.530	108.060	0.004	1.637
C2	83.640	158.760	91.220	0.002	1.933
C3	248.090	307.100	176.800	0.004	1.230

The response of the structure to the load can be seen in Figures 2 through 11 below:

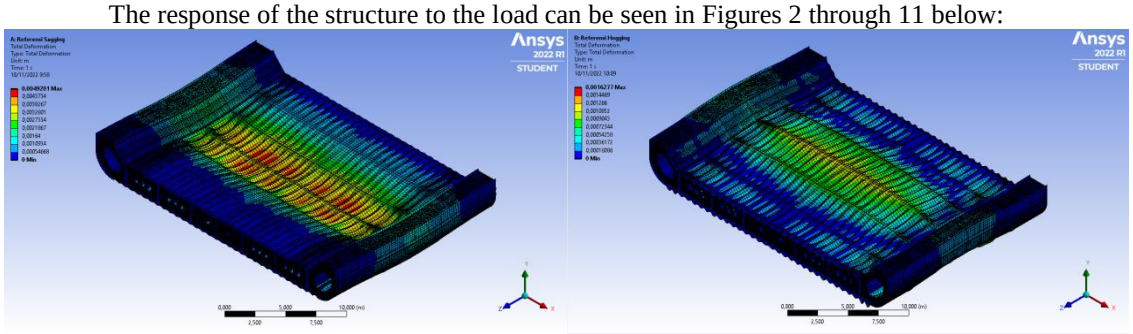

(a) (b)

Figure 2. Simulation results of the existing model: (a) sagging conditions, (b) hogging conditions

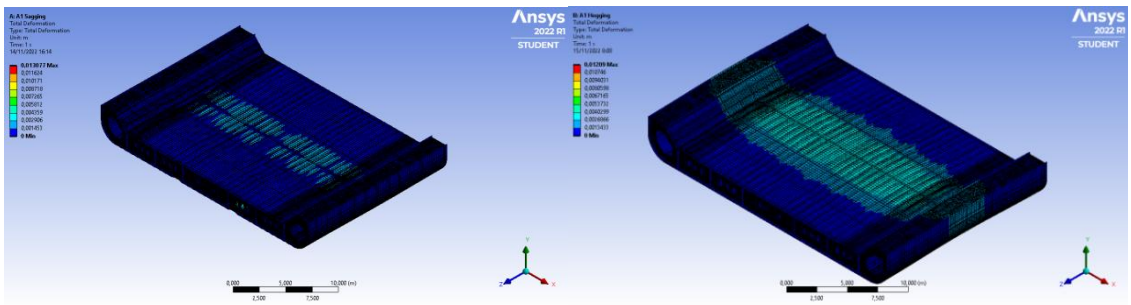

(a) (b)

Figure 3. Simulation results of the A1 model:(a) sagging conditions, (b) hogging conditions

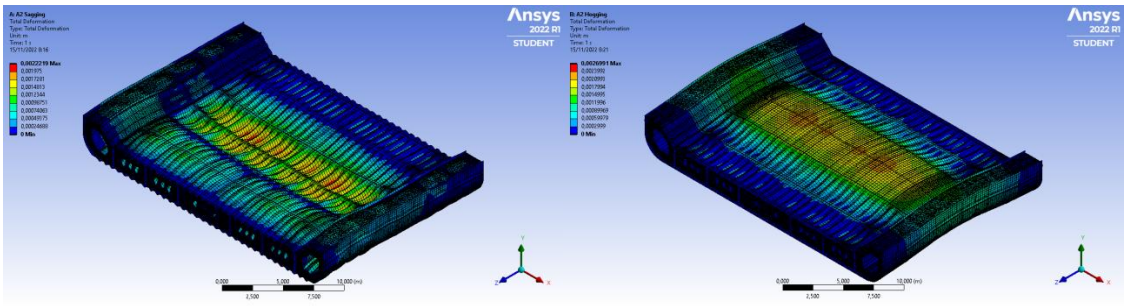

(a) (b)

Figure 4. Simulation results of the A2 model: (a) sagging conditions, (b) hogging conditions

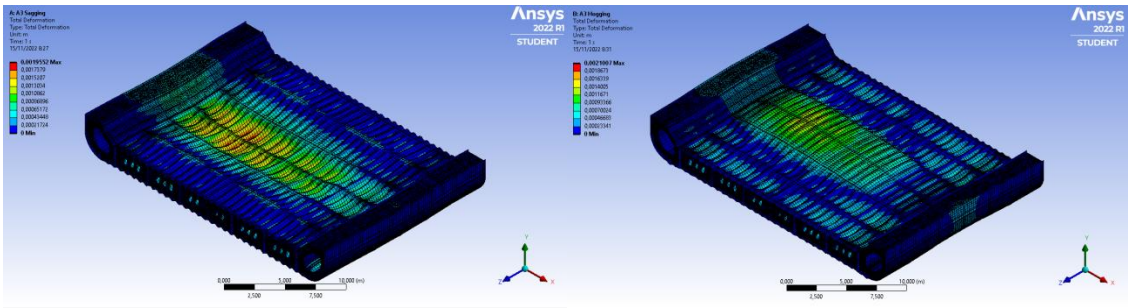

(a) (b)

Figure 5. Simulation results of the A3 model: (a) sagging conditions, (b) hogging conditions

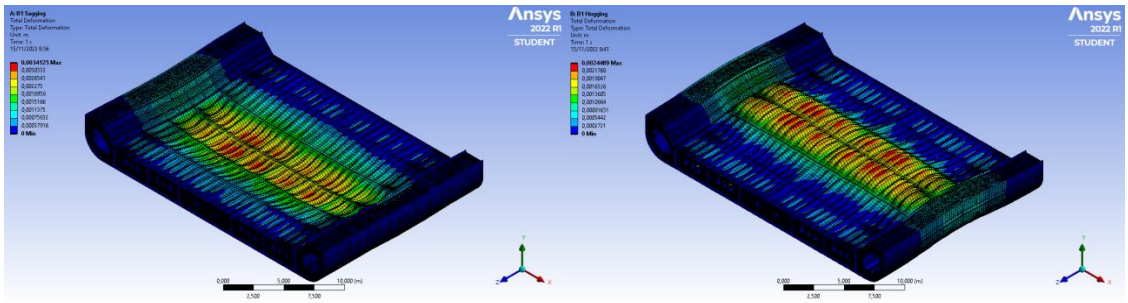

(a) (b)

Figure 6. Simulation results of the B1 model: (a) sagging conditions, (b) hogging conditions

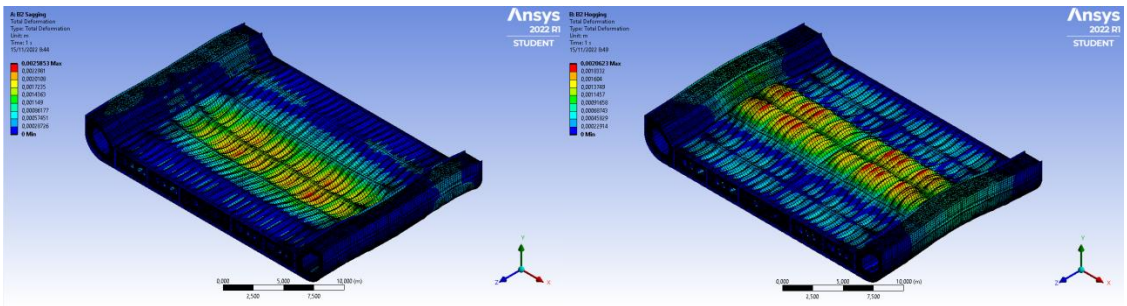

(a) (b)

Figure 7. Simulation results of the B2 model: (a) sagging conditions, (b) hogging conditions

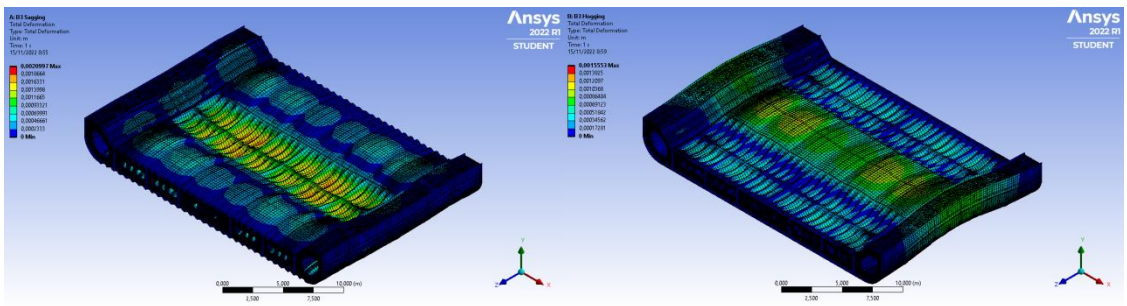

(a) (b)

Figure 8. Simulation results of the B3 model: (a) sagging conditions, (b) hogging conditions

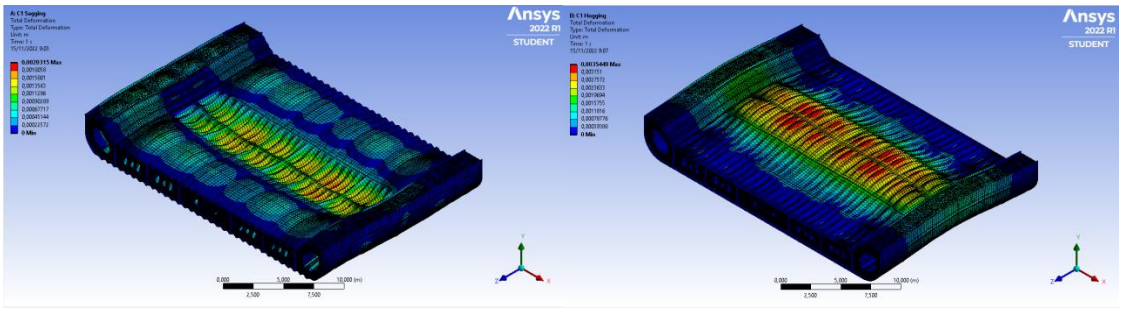

(a) (b)

Figure 9. Simulation results of the C1 model: (a) sagging conditions, (b) hogging conditions

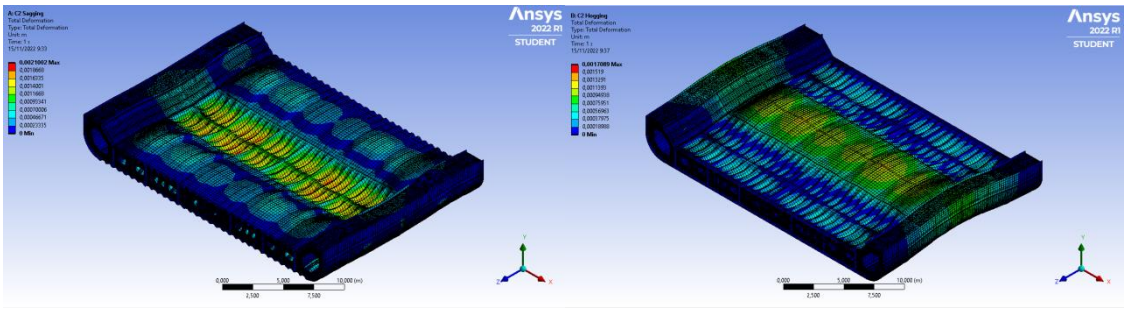

(a) (b)

Figure 10. Simulation results of the C2 model: (a) sagging conditions, (b) hogging conditions

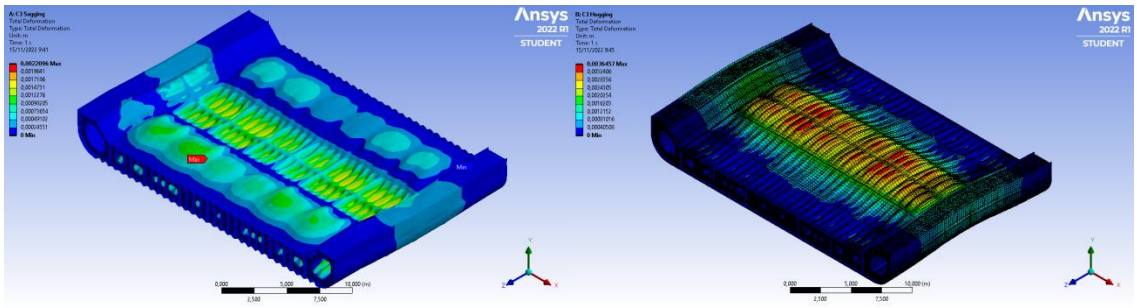

(a) (b)

Figure 11. Simulation results of the C3 model: (a) sagging conditions, (b) hogging conditions

Based on the results of manual calculations, the following data is obtained:

1. Permissible stress
   The results of the calculation of the permissible stress based on BKI volume II section 5 D.1.2 of 2017 (equation 2) are as follows:
   σ_{permit} = 248,213 MPa
   σ_{permit} is limit maximum stress based BKI. Meanwhile, in the mechanical engineering calculation permissible stress chose based yield strength from material specification (307 MPa) [12].

2. Maximum stress
   The maximum stress is calculated based on the following equation [14]:

   $$\sigma_{maks} = MT/WB \quad (3)$$

   where,
   MT = moment total [kN.m]
   WB = section modulus double bottom [m3]
   Based on the calculation results, the following data is obtained:
   MT = (-)4243968.357 kN.m (sagging)
   MT = 884589.952 kN.m (hogging)
   WB = 18.189 m3
   So the maximum stress value is:
   σmaks = 233,314 MPa (sagging)
   σmaks = 154,892 MPa (hogging)

3. Von mises stress
   The calculation of the von Mises stress is carried out using the theory of distortion energy (von Mises). This theory explains that failure is predicted to appear under multiaxial stress conditions when the distortion energy per unit volume becomes equal to or exceeds the distortion energy per unit volume at the time of failure of the test material [15]. The equation of this theory is as follows:

   $$\sigma_{eq} = \frac{\sqrt{2}}{2}[(\sigma_x - \sigma_y)^2 + (\sigma_y - \sigma_z)^2 + (\sigma_z - \sigma_x)^2 + 6(\tau_{xy}^2 + \tau_{yz}^2 + \tau_{zx}^2)]^{0.5} \quad (4)$$

   Based on the calculation results, the von mises stress obtained sequentially from the existing model to the C3 model for sagging condition is 228.200 MPa, 273.675 MPa, 169.609 MPa, 271.289 MPa, 238.429 MPa, 223.457 MPa, 248.286 MPa, 195.116 MPa, 248.147 MPa, 236.735 MPa. Meanwhile, the results

von mises stress for hogging condition is 134.809 MPa, 242.205 MPa, 206.775 MPa, 182.562 MPa, 196.911 MPa, 251.888 MPa, 107.478 MPa, 187.741 MPa, 158.679 MPa, 306.579 MPa.

4. Shear stress
   The calculation of shear stress is done using the theory of maximum shear stress (Tresca). This theory explains that a material that is loaded with biaxial or triaxial stress is declared to have failed if the maximum shear stress that occurs at each point reaches the shear yield stress of the material [15]. The equation of this theory is as follows:

$$\tau\ maks = \pm\sqrt{\left(\frac{\sigma_X - \sigma_Y}{2}\right)^2 + (\tau_{XY})^2} \quad (5)$$

   Based on the calculation results, the shear stress value is obtained as follows:
   τ_{maks} = 137,493 MPa

The validation results for maximum stress versus allowable stress for sagging conditions are satisfactory for all models. The highest maximum stress occurs in the existing model, which is 236,600 MPa. Meanwhile, the lowest maximum stress occurs in model B3, which is 125.770 MPa. The validation of the maximum stress against the allowable stress under the hogging conditions was compliant with all models except the A1 model. The maximum stress that meets the highest standard occurs in the C3 model, which is equal to 248.090 MPa. The lowest maximum stress occurs in model B3, which is 83,600 MPa. The results of validating the maximum stress on the calculated stress in the existing model with sagging hogging conditions each have a value of 0.014 and 0.054. The validity value between the simulation and the calculation in the sagging condition is the highest at 0.003 for the A1 model. The validity value with the largest difference occurs in the B3 model, which is 0.461. Meanwhile, the highest value of the validity of the hogging condition was in the A2 model, namely 0.010. The validity value with the largest difference occurs in model A1, which is 0.432.

The results of the validation of the von Mises stress against the allowable stress under the sagging condition complied with all models. The highest von Mises stress occurs in model B3, which is 238.720 MPa. Meanwhile, the lowest von Mises stress occurred in model A2, which was 190.720 MPa. The validation of the von Mises stress against the allowable stress under the hogging condition complies with all models except model B2 and model C3. The highest von Mises stress occurs in model A1, which is 242.180 MPa. The lowest von Mises stress occurs in model B3, which is 106.520 MPa. The results of the von Mises stress validation on the existing model with sagging hogging conditions each have a value of 0.001 and 0.011. the validity value between the simulation and the calculation at the smallest sagging condition for models C1 and C3. The validity value with the largest difference occurs in model A2, which is 0.111. Meanwhile, the validity value of the von Mises stress in the hogging condition is the highest in model A1. The validity value with the largest difference occurs in model A2, which is 0.29.

The results of the validation of shear stress against the allowable stress under the sagging condition complied with all models. The highest shear stress occurs in model A3, which is 156.420 MPa. Meanwhile, the lowest shear stress occurred in model A2, which was 97.590 MPa. Validation of the shear stress against the allowable stress under hogging conditions complies with all models. The highest shear stress occurs in model B2, which is 145.180 MPa. The lowest shear stress occurs in model B3, which is 61.470 MPa. The results of the validation of shear stress against the calculated stress in the existing model with sagging hogging conditions each have a value of 0.044 and 0.437. The validity value between the simulation and the calculation in the sagging condition is the highest at 0.001 for the B1 model. The validity value with the largest difference occurs in model A2, which is 0.290. Meanwhile, the validity value of the shear stress in the hogging condition is the highest in model A1, which is 0.015. The validity value with the largest difference occurs in the B3 model, which is 0.553.

B. Discussion

The results of the calculation of construction weight planning for each variable and model tend to decrease. This is in line with the research objective of reducing the construction weight of the existing model. The reduced weight of the construction is due to the reduced area of the floor plate due to the addition of variations in the size of the manhole. However, the reduction in the construction weight of each model compared to the existing model is not that significant. This happens because each increase in the size or number of manholes must also be added to the stiffener profile as reinforcement. The results of the construction weight calculation can be seen in Table 7 below:

TABLE 7.
DOUBLE BOTTOM CONSTRUCTION WEIGHT

Model	Construction weight (tons)
existing	201,831
A1	201,768
A2	201,740
A3	201,401
B1	201,532
B2	200,074
B3	199,925
C1	201,476
C2	199,495
C3	199,272

The maximum stress value in sagging and hogging conditions is generally relatively reduced. This is due to variations in the area of the floor plate used as a support for the double-bottom construction. The stress value that works is linear with the percentage value of the plate area reduction [16]. In addition, the support of the stiffener plates against the floor plate also affects the maximum strength of the model, where the holes that have stiffener plates have a better maximum strength [2]. The simulation results show that providing a stiffener around the hole can minimize the maximum stress reduction and bending in the hole area due to loading. The placement of holes in the floor plate must also be considered to obtain maximum construction strength [7].

The value of the von Mises stress in sagging and hogging conditions varies quite a bit between models. There is no fixed analysis for whether there is an increase or decrease in the von Mises stress due to variations in the existing model. In some models, there is an increase in the von Mises stress compared to the existing model. The results showed that the addition of plate hole dimensions can increase the von Mises stress on the plate [16]. Based on the von Mises theory, it is explained that the material will yield or break if the applied load produces a von Mises stress that exceeds the yield point of the material [15]. This means that the von Mises stress provides information about the yield or fracture limit of a material, while the principal stress is the actual stress acting on each principal plane or model. The von Mises stress is also affected by the size of the support construction [17]. This also causes variations in the simulation results.

According to the theory of shear stress (tresca), failure will occur if the shear stress that occurs in the material is equal to or greater than the maximum stress in the material yield condition [15]. Based on the simulation results, it is known that the value of the maximum shear stress is still below the maximum yield stress, meaning that the strength of the construction in the model is still quite safe. In many parts of the ship, the longitudinal pressure is the most dominant component. However, under certain conditions in the cross section, the shear stress component becomes significant [18]. Based on the results of the analysis, it show that the longitudinal stiffener is the most dominant area for shear stress. In addition, another area where there is maximum shear stress is on the floor plate.

The deformation resulting from the simulation can be seen based on the primary response, secondary response, and tertiary response of the stomach [4]. The primary response is the response of the entire hull when the ship bends under the longitudinal pressure of the ship. The primary response is usually called the ship's longitudinal bending stress. Meanwhile, the secondary response is related to the response or bending of the plate or stiffener on the double bottom, double side, and double hull ships. The tertiary response is related to the response to the skin plate due to loading [18]. Based on the results of the analysis, it is known that the deformation that occurs is a secondary and tertiary response of the model. The simulation results can be seen in Figures 12 and 13 below

.

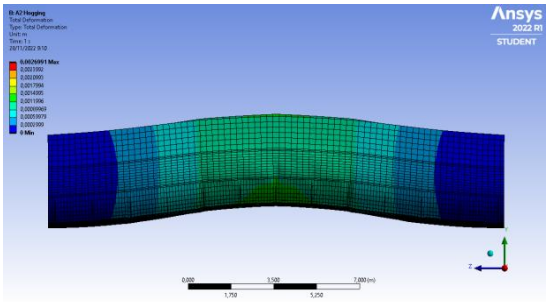

Figure 12. Secondary response simulation model

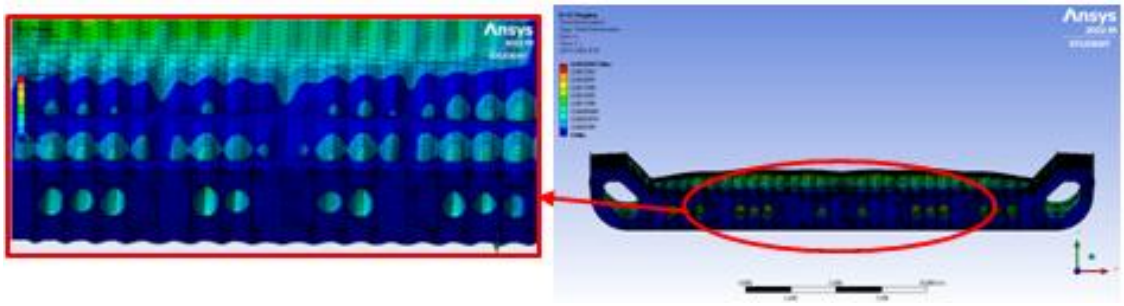

Figure 13. Tertiary response simulation model

Based on the results of the analysis using the SAW (Simple Additive Weighting) decision-making system method, it is found that the maximum stress is most effective in model B1. In the condition of sagging, the

maximum stress produced is 186.930 MPa, which is reduced by 20% from the existing model. This figure is still acceptable when viewed from the perspective of the maximum allowable stress. The validity value between the simulated stress and the calculated stress is 0.199. The resulting safety factor is 1.337. The safety factor value is acceptable because it is still above 1. Meanwhile, in the hogging condition, the maximum stress generated by model B1 is 141.540 MPa, down 8.20% from the existing model. The validity value between the simulated stress and the calculated stress is 0.030. The resulting safety factor is 2.119. The safety factor value is still acceptable because it is still above 1.

The results of the von Mises stress analysis using the same method are most effective in model B1. In the von Mises stress sagging condition, the output is 238.720 MPa, an increase of 4.52% from the existing model. The validity value between the simulated stress and the calculated stress is 0.121. The resulting safety factor is 1.337. The safety factor value is acceptable because it is still above 1. Meanwhile, in the hogging condition, the von Mises stress produced by model B1 is 184.820 MPa, an increase of 26.27% from the existing model. The validity value between the simulated stress and the calculated stress is 0.119. The resulting safety factor is 2.119. The safety factor value is still acceptable because it is still above 1.

The results of shear stress analysis using the same method were most effective in model B1. In the sagging condition, the resulting shear stress is 137.420 MPa, an increase of 4.31% from the existing model. The validity value between the simulated stress and the calculated stress is 0.001. The resulting safety factor is 1.337. The safety factor value is still acceptable because it is still above 1. Meanwhile, in the hogging condition, the shear stress produced by model B1 is 113.370 MPa, an increase of 31.76% from the existing model. The validity value between the simulated stress and the calculated stress is 0.20. The resulting safety factor is 2.11. The safety factor value is still acceptable because it is still above 1.

IV. CONCLUSION

Based on the results of the research and discussion above, it can be concluded as follows:

1) The results of the strength analysis of the existing double bottom model construction obtained maximum stress values in the sagging hogging condition of 236.60 MPa and 154.18 MPa. The von Mises stress values for the sagging hogging conditions are 227.94 MPa and 136.26 MPa, respectively. The shear stress values for the sagging hogging condition are 131.5 MPa and 77.36 MPa.
2) Based on the results of the analysis, variations in the design or shape of the manhole according to BKI rules are models A2, B1, and C1. The results of this analysis are based on the validation of the stress value in each parameter against the allowable stress from BKI. The results of the modification to the A2 model are the addition of 2 manhole holes with a size according to the existing model, namely 600 x 800 mm, a ratio of 0.75. The results of the modifications to the B1 model are the addition of a hole height of 200 mm from 600 x 800 to 600 x 1000 mm and a change in the hole ratio from 0.75 to 0.6. The results of the modifications to the C1 model are the addition of a hole height of 200 mm from 600 x 800 to 600 x 1000 mm and the addition of two manholes of similar size.
3) The effect of changing the shape or dimensionality of the manhole on the maximum stress is that the resulting stress value is linear with the percentage value of the reduction in the area of the plate or the variation of the manhole. The results of the analysis of the maximum stress in the sagging condition show that each model has experienced a reduction with an average percentage reduction of 23.817%. While in the hogging condition, there is a maximum stress reduction in models A2, B1, B3, and C2, with an average reduction percentage of 26.064%. The results of the von Mises stress analysis show that the addition of plate hole dimensions can increase the value of the von Mises stress on the plate. The results of the von Mises stress analysis under the sagging condition show that there is an increase in the stress value in models A1, A3, B1, B3, C2, and C3, with an average percentage increase of 11.129%. The von Mises stress in each model increases with a percentage of 43.462% while in the hogging condition. The effect of adding the dimensions of the manhole hole to the shear stress can increase the value of the shear stress. The results of the analysis of the shear stress under the sagging condition showed an increase in the value of the shear stress in models A1, A3, B1, B3, C2, and C3, with an average percentage increase of 9.26%. While in the hogging condition, there is an increase in shear stress in each model, with an average percentage increase of 52.222%. The results of the analysis show that the stress value is quite varied in each model compared to the existing model. This is due to the influence of the supporting construction components of the double bottom model.

This research can still be developed further by adding a more detailed analysis. The object of this research is an oil tanker ship with a size of 17,500 LDWT, so for ships of other sizes or types, it is necessary to make calculation adjustments based on the type of ship under study. The design of this research object model can be made even more complex by adding other parts of the ship, such as the side, deck, and other parts. The loading used in this research simulation can be further developed, such as when the ship is fully loaded or other loads are acting on it. The discussion analysis can be developed further by adding other parameters such as construction age analysis, analysis due to environmental influences such as corrosion, and so on.

ACKNOWLEDGMENTS

The author gives appreciation and thanks to the

Department of Naval Architecture, Faculty of Engineering, Jember University, and all Parties who helped complete this research. Hopefully, this research can provide benefits and can be developed in further research.

REFERENCES

[1] Djaya, I. K, 2008. Teknik Konstruksi Kapal Baja Jilid 1, Direktorat Pembinaan Sekolah Menengah Kejuruan, Jakarta.

[2] Cui, J., & Wang, D., 2020. An experimental and numerical investigation on ultimate strength of stiffened plates with opening and perforation corrosion. *Journal Ocean Engineering*, (205) pp. 1-16.

[3] Sanjaya, D. D., 2017. Analisa Kekuatan Konstruksi Wing Tank Kapal, *Tugas Akhir*, Institut Teknologi Sepuluh Nopember, Surabaya.

[4] Mayo, 2015, Analytical And Numerical Determination Of The Hull Girder Deflection Of Inland Navigation Vessels Del Buque-Viga De Buques De Navegación Interior, Politeknik de Cartagena.

[5] BKI, 2017, Rules for the Classification and 2017 Edition Biro Klasifikasi Indonesia: Vol. II, Biro Klasifikasi Indonesia, Jakarta.

[6] Alamsyah, Wulandari, A. E., & Ramadhan, B. H., 2020, Analisa Kekuatan Bracket Pada Kapal Ro-Ro Menggunakan Aplikasi Finite Element. *SPECTA Journal of Technology*, Vol.4 (3), pp. 97–105.

[7] Piscopo, V., & Scamardella, A., 2021, Improved design formulas for the ultimate strength of platings with circular openings and manholes under uniaxial compression, *Journal Marine Structures*, (75), pp. 1-18.

[8] Chen, X., & Liu, Y., 2015, Finite Element Modelling and Simulation with ANSYS Workbench, CRC Press, New York.

[9] Permana, I., & Setyawan, D., 2019, Analisis Kekuatan Konstruksi Alas Kapal Akibat Grounding. *Jurnal Teknik ITS*, Vol. 8 (2), pp. 151–158.

[10] Ardianto, R. Y., 2017, Analisis Tegangan Geser pada Struktur Kapal Bulk Carrier dengan Dua Lubang Palkah Tiap Ruang Muat, *Thesis*, Institut Teknologi Sepuluh Nopember, Surabaya.

[11] Ramadhan, A., Mulyatno, I. P., & Yudo, H., 2016, Analisa Kekuatan Konstruksi Double Bottom Pada Frame 46 Sampai Frame 50 Akibat Perubahan Dari Single Hull Ke Double Hull Pada Kapal Tanker 13944 LTDW dengan Metode Elemen Hingga, *Jurnal Teknik Perkapalan*, Vol. 4 (4), pp. 858–867.

[12] Mubarak, A. A., 2019, Kekuatan Batas Lambung Kapal Dalam Menahan Momen Lentur Vertikal, *Jurnal Penelitian Enjiniring*, Vol. 22 (1), pp. 56–61.

[13] Prastyo, Y., Mulyatno, P., & Yudho, H., 2016, Analisa Kekuatan Konstruksi Modifikasi Double Bottom Akibat Alih Fungsi Pada Kapal Accomodation Work Barge (Awb) 5640 Dwt Dengan Metode Elemen Hingga. *Jurnal Teknik Perkapalan*, Vol. 4 (1). Pp. 83-90.

[14] Makmun, S., 2017, Studi Penilaian Kekuatan Buckling Pelat pada Struktur Kapal Menggunakan Aturan BKI, *Jurnal Teknik BKI Technical Journal of Classification and Independent Assurance*. Vol. 4, pp. 49-58.

[15] Hibbler, R. C., 2015, Mechanics of Materials 8 Th Edition, Pearson, New York.

[16] Alamsyah, Wulandari, A. E., & Ramadhan, B. H., 2020, Analisa Kekuatan Bracket Pada Kapal Ro-Ro Menggunakan Aplikasi Finite Element, *SPECTA Journal of Technology*, Vol. 4 (3), pp. 97–105.

[17] Saad-Eldeen, S., Garbatov, Y., & Guedes Soares, C., 2018, Structural capacity of plates and stiffened panels of different materials with opening, *Journal Ocean Engineering*, Vol. 167, pp. 45–54.

[18] Rigo, P., & Rizzuto, E., 2010, Analysis and Design of Ship Structure, *Ship Design and Construction*, pp. 1–37.